



HAL
open science

Safe Polycationic Dendrimers as Potent Oral In Vivo Inhibitors of *Mycobacterium tuberculosis*: A New Therapy to Take Down Tuberculosis

Serge Mignani, Vishwa Deepak Tripathi, Dheerj Soam, Rama Pati Tripathi, Swetarka Das, Shriya Singh, Ramakrishna Gandikota, Regis Laurent, Andrii Karpus, Anne-Marie Caminade, et al.

► To cite this version:

Serge Mignani, Vishwa Deepak Tripathi, Dheerj Soam, Rama Pati Tripathi, Swetarka Das, et al.. Safe Polycationic Dendrimers as Potent Oral In Vivo Inhibitors of *Mycobacterium tuberculosis*: A New Therapy to Take Down Tuberculosis. *Biomacromolecules*, 2021, 22 (6), pp.2659-2675. 10.1021/acs.biomac.1c00355 . hal-03273968

HAL Id: hal-03273968

<https://hal.science/hal-03273968>

Submitted on 14 Oct 2021

HAL is a multi-disciplinary open access archive for the deposit and dissemination of scientific research documents, whether they are published or not. The documents may come from teaching and research institutions in France or abroad, or from public or private research centers.

L'archive ouverte pluridisciplinaire **HAL**, est destinée au dépôt et à la diffusion de documents scientifiques de niveau recherche, publiés ou non, émanant des établissements d'enseignement et de recherche français ou étrangers, des laboratoires publics ou privés.

Safe polycationic dendrimers as potent oral *in vivo* inhibitors of *Mycobacterium tuberculosis*: A new therapy to take down tuberculosis

Serge Mignani^{*a,b}, Vishwadeepak Tripathi,^{c,d} Dheerj Soam^e, Rama P Tripathi^{*f}, Swetarka Das^e, Shriya Singh^e, Ramakrishna Gandikota^{c,d}, Regis Laurent^{c,d}, Andrii Karpus^{c,d}, Anne-Marie Caminade^{c,d}, Anke Steinmetz^g, Arunava Dasgupta^{*h}, Kishore K Srivastava^{*h}, Jean-Pierre Majoral^{*c,d},

- (a) Université Paris Descartes, PRES Sorbonne Paris Cité, CNRS UMR 860, Laboratoire de Chimie et de Biochimie Pharmacologiques et Toxicologique, 45, rue des Saints Peres, 75006 Paris, France. Email : serge.mignani@parisdescartes.fr and serge.mignani@staff.uma.pt
- (b) CQM - Centro de Química da Madeira, MMRG, Universidade da Madeira, Campus da Penteada, 9020-105 Funchal, Portugal
- (c) Laboratoire de Chimie de Coordination du CNRS, 205 Route de Narbonne, BP 44099, 31077 Toulouse CEDEX 4, France Email : jean-pierre.majoral@lcc-toulouse.fr
- (d) LCC-CNRS, Université de Toulouse, CNRS, Toulouse, France
- (e) Microbiology Division, CSIR-Central Drug Research Institute, Lucknow, India
- (f) Medicinal and Process Chemistry Division, CSIR-CDRI Lucknow, India Email: rpt.cdri@gmail.com
- (g) Sanofi R&D, Integrated Drug Discovery, Centre de Recherche Vitry-Alfortville, 94403 Cedex Vitry-sur-Seine, France;
- (h) Microbiology Division, CSIR-Central Drug Research Institute, B.S. 10/1, Sector 10, Janakipuram Extension, Sitapur Road, Lucknow - 226031, India Email: a.dasgupta@cdri.res.in (AD), kishore@cdri.res.in (KS)

KEYWORDS

Dendrimers, Polycationic phosphorus dendrimers, Mycobacterium tuberculosis, *M. tuberculosis* H37Ra, *M. tuberculosis* H37Rv and *M. Bovis* BCG, Anti-mycobacterial activity

ABSTRACT

The long-term treatment of tuberculosis (TB) sometimes leads to non-adherence to treatment resulting in multi drug resistant (MDR) and extensively drug-resistant (XDR) tuberculosis. Inadequate bioavailability of the drug is the main factor for therapeutic failure which leads to the development of drug-resistant cases. Therefore, there is an urgent need to design and develop novel anti-mycobacterial agents minimizing the period of treatment and reducing the propagation of resistance at the same time. Here, we report the development of original and non-cytotoxic polycationic phosphorus dendrimers essentially of generations 0 and 1, but also of generations 2 to 4, with pyrrolidinium, piperidinium and related cyclic amino groups on the surface, as new anti-tubercular agents active *per se*, meaning with intrinsic activity. The strategy is based on the phenotypic screening of a newly designed phosphorus dendrimer library (generation 0 to 4) against three bacterial strains: attenuated *M. tuberculosis* H37Ra, virulent *M. tuberculosis* H37Rv, and *M. bovis* BCG. The most potent polycationic phosphorus dendrimers **1G0,HCl** and **2G0,HCl** are active against all three strains with MICs between 3.12 and 25.0 µg/ml. Both are irregularly shaped nanoparticles with highly mobile branches presenting a radius of gyration of 7 Å, a diameter of maximal 25 Å, and a solvent-accessible surface area of dominantly positive potential energy with very localized negative patches arising from the central N₃P₃ core which steadily interacts with water molecules. The most interesting is **2G0,HCl** showing relevant efficacy against single drug resistant (SDR) *M. tuberculosis* H37Rv, resistant to Rifampicin, Isoniazid, Ethambutol, or Streptomycin. Importantly, **2G0,HCl** displayed significant *in vivo* efficacy based on bacterial counts in lung of infected Balb/C mice at the dose of 50 mg/kg oral administration once a day

for two weeks, and superior efficacy in comparison to Ethambutol and Rifampicin. This series of polycationic phosphorus dendrimers represents first-in-class drugs to treat TB infection, could fulfill the clinical candidate pipe of this high burden of infectious disease, and play a part in the continuous demand for new drugs.

INTRODUCTION

Throughout history, the disease of tuberculosis has been known by different names: consumption, phtharmia, and white plague. Cristóbal Rojas (1857-1890) was suffering from tuberculosis and painted the famous “La Miseria” in 1886. In it he depicts the social aspect of the disease and its relationship with living conditions at the end of the 19th century. Tuberculosis (TB) is a contagious, airborne infectious disease caused most commonly by infection with various pathogen strains of mycobacteria, such as *Mycobacterium tuberculosis* (MTB), and is a major public health burden. MTB is a small aerobic non-motile bacillus. According to the World Health Organization (WHO), an estimated 10 million people fell ill with TB in 2019. This number has been declining very slowly in recent years.¹ There were close to 1.4 million and 208,000 TB deaths among HIV-negative and HIV-coinfected patients, respectively.¹ Eight countries accounted for two thirds of the global total: India (26%), Indonesia (8.5%), China (8.4%), the Philippines (6.0%), Pakistan (5.7%), Nigeria (4.4%), Bangladesh (3.6%), and South Africa (3.6%).¹ Despite the great reduction of incidence and mortality rate over the years, the current challenge is the increase of the prevalence of multidrug-resistant TB (MDR-TB) and extensively drug-resistant TB (XDR-TB), a form of TB which is resistant to at least four of the core anti-TB drugs, since the introduction of several types of drugs. In 2016, an estimated 490,000 people worldwide developed MDR-TB.¹ Consequently, TB represents a tough challenge and a public health threat. Moreover, according to the WHO, the recent Covid-19 pandemic threatens to reverse the progress made in recent years in the fight against tuberculosis. As a result, the countries most affected by tuberculosis are focusing more on Covid-19 detection than on TB detection. According to the WHO annual report, TB could cause 200,000 to 400,000 more deaths this year than the 1.4 million in 2019, despite the existence of a cure.¹

Effective treatment is difficult due to the specific structure and chemical composition of the mycobacteria cell wall hindering the entry of drugs, which renders many drugs and antibiotics

ineffective. However, the antibiotics isoniazid, rifampicin, pyrazinamide, ethambutol, and streptomycin are the major first-line pulmonary anti-TB drugs that are all typically applied as 6 months treatment.² The majority of anti-TB drugs are administered orally except *Streptomycin*, *Amikacin*, *Kanamycin*, and *Capreomycin* which are administered intravenously. Poor patient compliance to prescribed regimens and the emergence of resistant strains are the major problems during TB long-term treatment, which involves continuous, frequent multiple drug dosing. At this point, two strategies have been developed: 1) shortening the treatment duration and reducing the dosing frequency with the capacity to tackle drug-resistant TB; 2) developing new drug formulations to reduce toxic side effects. Indeed, the introduction of long-duration drug formulations that release antimicrobial agents - incorporating both hydrophilic and hydrophobic substances - in a slow and sustained manner, allowing the reduction in frequency and total number of doses, represents an important therapeutic strategy against TB.³ In this direction, several stable nanoparticle-based formulations for the controlled and sustained release of first-line anti-TB drugs such as isoniazid, rifampin, and pyrazinamide have been described and show good efficiency in *in vivo* models. For instance, poly-lactide-co-glycolide (PLG) nanoparticles, lectin-functionalized PLG nanoparticles, and solid lipid nanoparticles were developed by the oral, subcutaneous, or aerosol route of administration.⁴ Recently, several nanoparticles for the delivery of anti-TB drugs directly to the lungs via the respiratory route have been analyzed. Globally speaking, the main advantages using nanoparticles, *e.g.* lipids, polymers, and proteins, in inhaled anti-TB drug delivery are as follows: 1) direct drug delivery in the lung targeting alveolar macrophages; 2) decreased risk of systemic toxicity; 3) delivery of multiple drugs simultaneously; 4) shortened treatment regimen; and 5) improved patient compliance.⁵ The cost of treatment, stability, and large-scale production of drug formulations are the main issues to be analyzed to bridge the gap between theory and clinical reality.⁶

Taken together, there is an urgent need for new efficacious and affordable chemotherapeutics with higher efficacy which is the main cause for failures in clinical drug development.^{7,8}

Recently, an interesting review highlighted the development of nanoparticles in TB treatment.⁹ Two strategies have been developed 1) antimycobacterial activities based on intrinsic activities; 2) nanoparticles as nanocarriers of known antitubercular drugs for oral or pulmonary administrations. Silver, gold, iron, iron oxide, and gallium nanoparticles targeting macrophages were used *in vitro* and *in vivo* with intrinsic antimycobacterial, in addition to anti-bacterial activity. Achievement of

biodegradable profiles is the main challenge. Several of these nanoparticles are coated, for instance, with polyacrylic acid and polysaccharide (chitosan). PLG wheatgerm agglutinin-coated PLG, poly lactic-co-glycolic acid (PLGA), chitosan, and gelatin are the main nanocarriers used, whereas rifampicin, isoniazid, pyrazinamide, ethambutol are the main drugs for both, oral and pulmonary delivery. In addition, several surface functionalized nanoparticles, such as gelatin, cationic lipids, and PLGA coated with mannose, lactose, mycolic acids, and PEG, with carried drugs such as isoniazid, rifampicin, and moxifloxacin were developed for antimycobacterial drug delivery.

To the best of our knowledge, no report emphasized the development of dendrimers which can be considered as soft nanoparticles, as drug *per se* against TB. Earlier work has described the use of dendrimers as nanocarriers, and was highlighted in several reviews.^{10,11} Dineshkumar *et al.* described the long-duration release of Rifampicin loaded PEGylated PAMAM dendrimers,¹² whereas R. Bellini *et al.* showed the high stability of the Rifampicin-PAMAM complex under physiological pH and the rapid release of Rifampicin molecules under acidic medium which is similar to the acidic domains of the macrophage where the Mycobacterium resides.¹³ Interestingly, Jain *et al.* described the intracellular macrophage uptake of Rifampicin loaded mannosylated PPI dendrimers,¹⁴ whereas N. Singh *et al.* used the same dendrimers for delivery of Isoniazid.¹⁵ A recent review has emphasized these new ways to treat tuberculosis using dendrimers as nanocarriers.¹⁶

Dendrimers are three-dimensional macromolecules with a high degree of molecular uniformity and a perfectly controlled shape, surface chemistry, and size in the range of 1–15 nm. A wide range of literature about dendrimers is available today.¹⁷ They display dendritic branches composed of hydrophobic and hydrophilic moieties radiating out from a central core unit. Interior layers generations, Gn (G), where n ranges generally from 1 to 6 and more exceptionally to 12 and even 13 are made of regularly repeating branching units attached to the core. The dendrimer diameter increases non-exponentially, whereas the number of surface groups increases exponentially for each generation. Because of their highly-branched, three-dimensional architecture and versatile surface functionalization, dendrimers have been engineered for use as nanodevices, either nanocarrier drug approaches¹⁸, or drugs *per se*.¹⁹

For several years, Majoral, Caminade, and co-workers have developed biocompatible phosphorus dendrimers, which represent a versatile platform in drug delivery, *e.g.*, drug and gene transfection delivery, as well as drugs themselves.²⁰ The high level of control that is possible over their architectural design, allowing for tunable control of sizes and shapes of cores and interiors as well as

tunable surface functionality are the main advantages of phosphorus dendrimers. Phosphorus dendrimers have been employed as drugs *per se* in different therapeutic fields as, for instance, anticancer,²¹ anti-prions,²² anti-Alzheimer's,²³ anti-inflammatory agents,²⁴ etc. In addition, a large variety of administration routes can be used with dendrimers in general and phosphorus dendrimers in particular: intravenous, intraperitoneal, ocular, transdermal, oral, intranasal, and pulmonary routes.²⁵ The latter is very important in the case of TB, because TB is caused by *Mycobacterium tuberculosis* bacteria that most often affect the lungs.

Herein, we report the development of original non-cytotoxic polycationic phosphorus dendrimers as new antitubercular agents active *per se*, meaning intrinsic *in vivo* activity. The strategy is based on the phenotypic screening of a newly designed phosphorus dendrimer library *versus*, for instance, target-based²⁶ or fragment-based approaches.²⁷ These intrinsically active nanoparticles represent *first-in-class* drugs to treat TB infection, to fulfil the clinical candidate pipe of this high burden of infectious disease, and to play a part in the continuous demand for new antitubercular drugs. We decided to develop nanoparticles in general and phosphorus dendrimers in particular due to three important points based on medical needs: 1) limited number of drugs to treat MDR-TB and XDR-TB, 2) substantial side effects including toxicity issues of drugs available, and 3) less effective second-line drugs. The antimycobacterial screening has been conducted against three bacterial strains: attenuated strain *M. tuberculosis* H37Ra, virulent *M. tuberculosis* H37Rv, and against *M. bovis* BCG.

SYNTHESIS OF DENDRIMERS

Our strategy for synthesis was to construct an original polycationic phosphorus dendrimer library of 27 members to evaluate the influence of the cationic moieties, the nature of the branches and the size (generations: Gn, n = 0, 1, 2, 3 and 4), on their antimycobacterial activity. The Figure 1 shows the general 2D structure of an example of polycationic phosphorus dendrimer of generation 1.

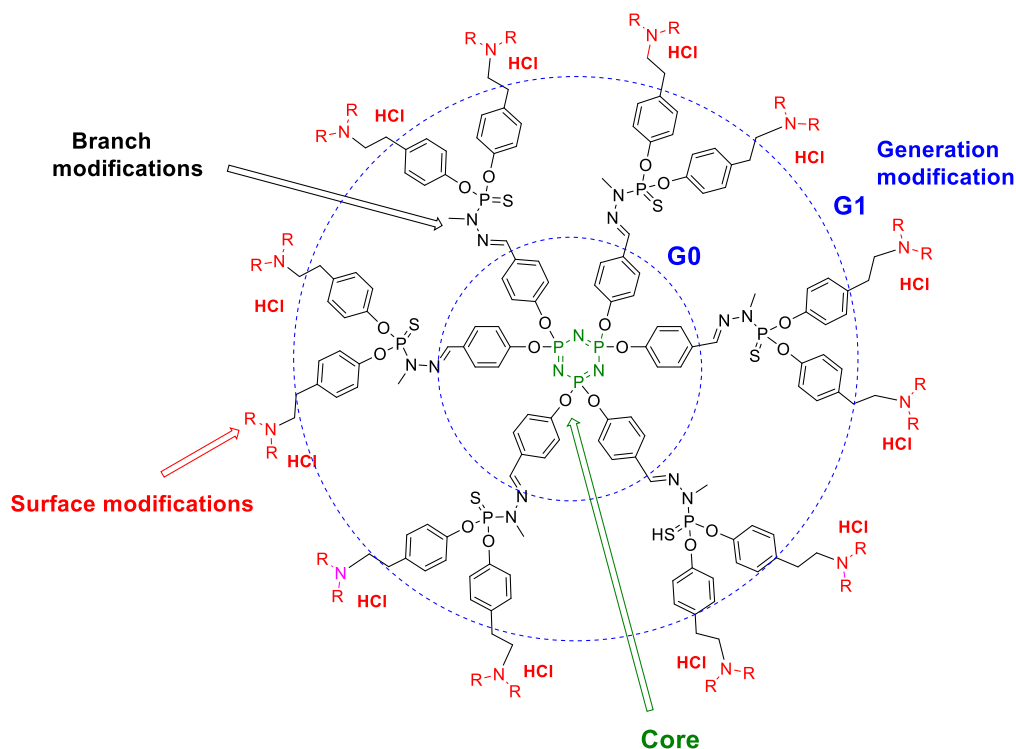
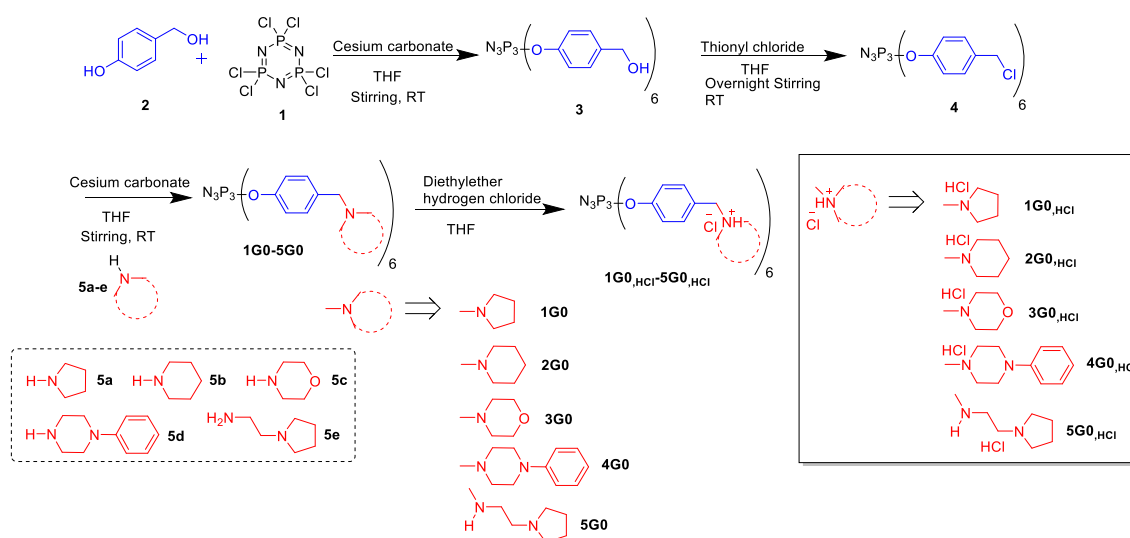


Figure 1. General 2D structure of an example of polycationic phosphorus dendrimer

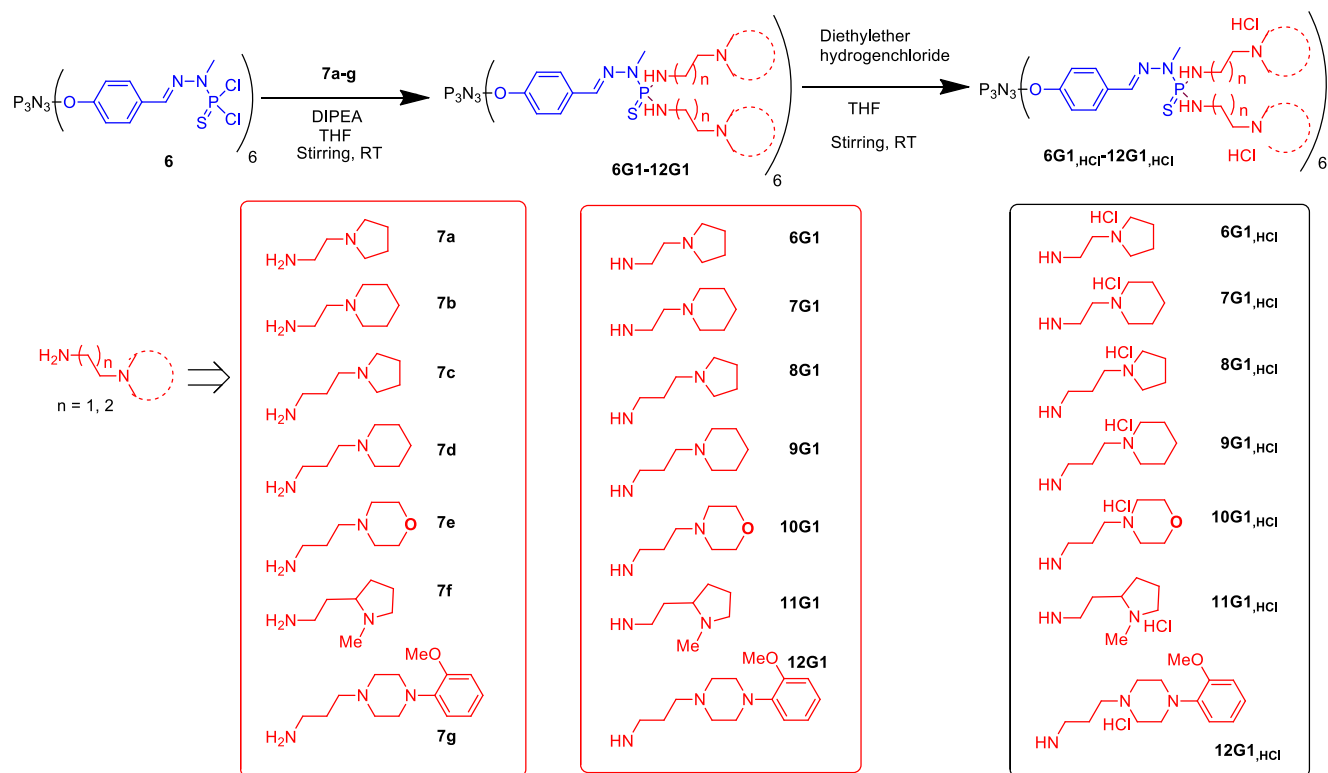
Pyrrolidino, *N*-methyl pyrrolidino, piperidino, *N*-methyl piperidino, morpholino, imidazolino, 1-phenyl-piperazino, pyrazine-2-carbonyl, and nicotinic groups have been introduced on the surface of phosphorus dendrimers in order to evaluate the influence of the cationic moieties on their antimycobacterial activity. The Tables 1-6 represent all the dendrimers prepared, classed by generation, and tested. The construction of these phosphorus dendrimers was also based on chemical feasibility and chemical stability, as well their aqueous solubility. The straightforward multistep synthesis has been adopted for the preparation of the phosphorus dendrimers of generation 0 (Scheme 1, compounds named **1G_{0,HCl}**-**5G_{0,HCl}**), generation 1 (Schemes 2 and 3, compounds named **5G_{1,HCl}**-**20G_{1,HCl}**, generation 2 (Scheme 5, **6G_{2,HCl}** and **7G_{2,HCl}**), generation 3 (Scheme 5, **6G_{3,HCl}**, **7G_{3,HCl}**) and generation 4 (Scheme 5, **6G_{4,HCl}** and **7G_{4,HCl}**, see supplementary materials). All compounds are first synthesized and characterized in the neutral form, which are named **XG_n**, with X being the number of the compound, and n being the generation (number of layers) of the dendrimer. The neutral dendrimers are generally less soluble in water, thus they are protonated (with HCl) to produce their corresponding water soluble dendrimers. These cationic dendrimers are named **XG_{n,HCl}**.

The Scheme 1 shows the preparation of dendrimers of generation 0 (compounds **1G0-5G0** and of their corresponding salt). In the first step, 4-hydroxybenzyl alcohol (**2**) is grafted to cyclotriphosphazene derivative $N_3P_3Cl_6$ in presence of cesium carbonate at room temperature to afford compound **3**. The six benzylalcohol groups are then converted to the benzylchloride **4** using thionyl chloride as chlorinating agent,²⁸ which is precursor of dendrimers **1G0-5G0**, by substitution of the chloride by diverse amines in presence of potassium carbonate at room temperature (**5a-e**) in good yields. Finally, water-soluble compounds are obtained (**1G0,HCl-5G0,HCl**) by adding 1 equiv. of HCl diethylether *per* terminal function (6 equiv. for the generation zero compounds).



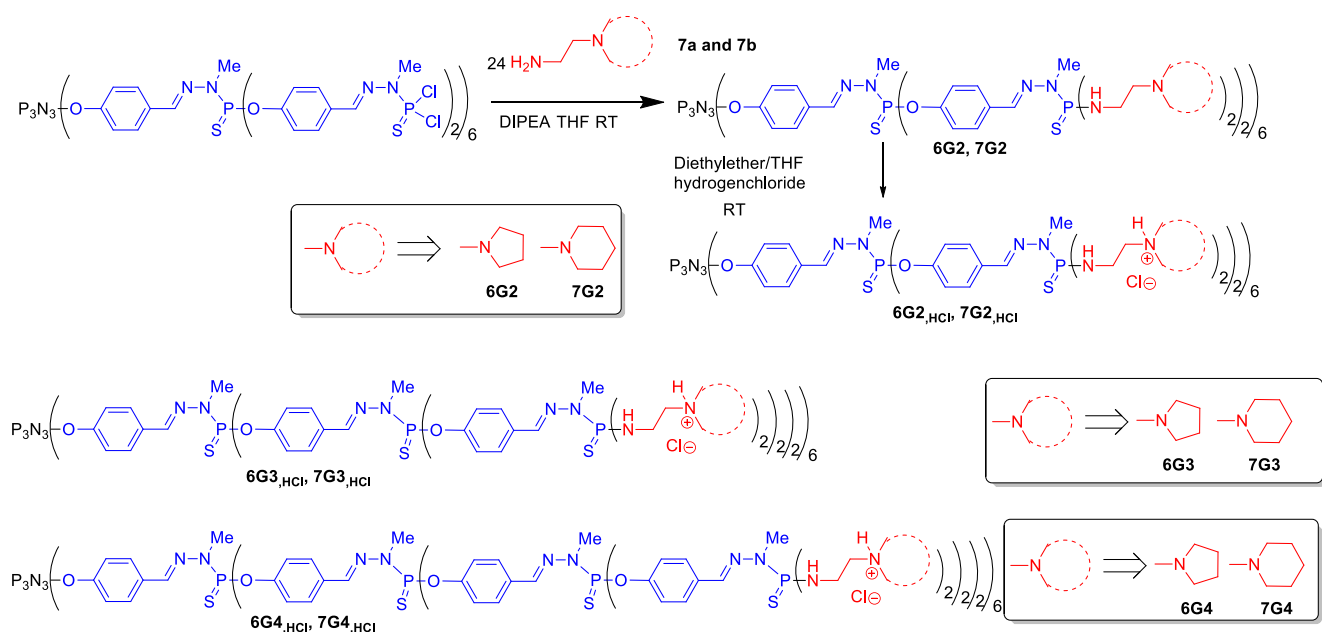
Scheme 1. General synthesis of **1G0,HCl-5G0,HCl** polycationic phosphorus dendrimers

The Scheme 2 highlights the general preparation of dendrimers of generation 1 (compounds **6G1-12G1** and of their respective salt). The starting point is the generation 1 dendrimer (**6**), built from the cyclotriphosphazene core^{29,30} The nucleophilic substitution with diverse primary amines (**7a-7g**) bearing through a C_2 or C_3 linker a cyclic amine as substituent³¹ in *N,N*-Diisopropyléthylamine (DIPEA) affords in good to excellent yields the dendrimers **6G1-12G1**. The corresponding water-soluble compounds (**6G1,HCl-12G1,HCl**) were obtained by adding 12 equiv. of HCl in diethylether to each dendrimer in quantitative yields.



Scheme 2. General synthesis of **6G1,HCl-12G1,HCl** polycationic phosphorus dendrimers

Scheme 3 shows the general synthesis of dendrimers of generation 1 (compounds **5G1**, **13G1-20G1** and of their corresponding salt). The first step is the simple condensation reaction at room temperature between the first-generation dendrimer functionalized with 12 aldehydes (compound **8**),^{30,31} with the amines **7a, b, e, f, h, i, j, k, l** several already used in Scheme 2. The second step is the reduction of the imine amines **9a, b, e, f, h, i, j, k, l** with NaBH_4 at room temperature; such reaction occurs only on the imines and not on the hydrazone linkages,^{32,33} affording dendrimers **5G1** and **13G1-20G1** in moderate to good yields. Protonation reaction has been carried out using 12 equiv. of HCl *per* dendrimer, even if at least 24 N *per* dendrimer could be protonated, affording **5G1,HCl** and **13G1,HCl-20G1,HCl** in quantitative yield.

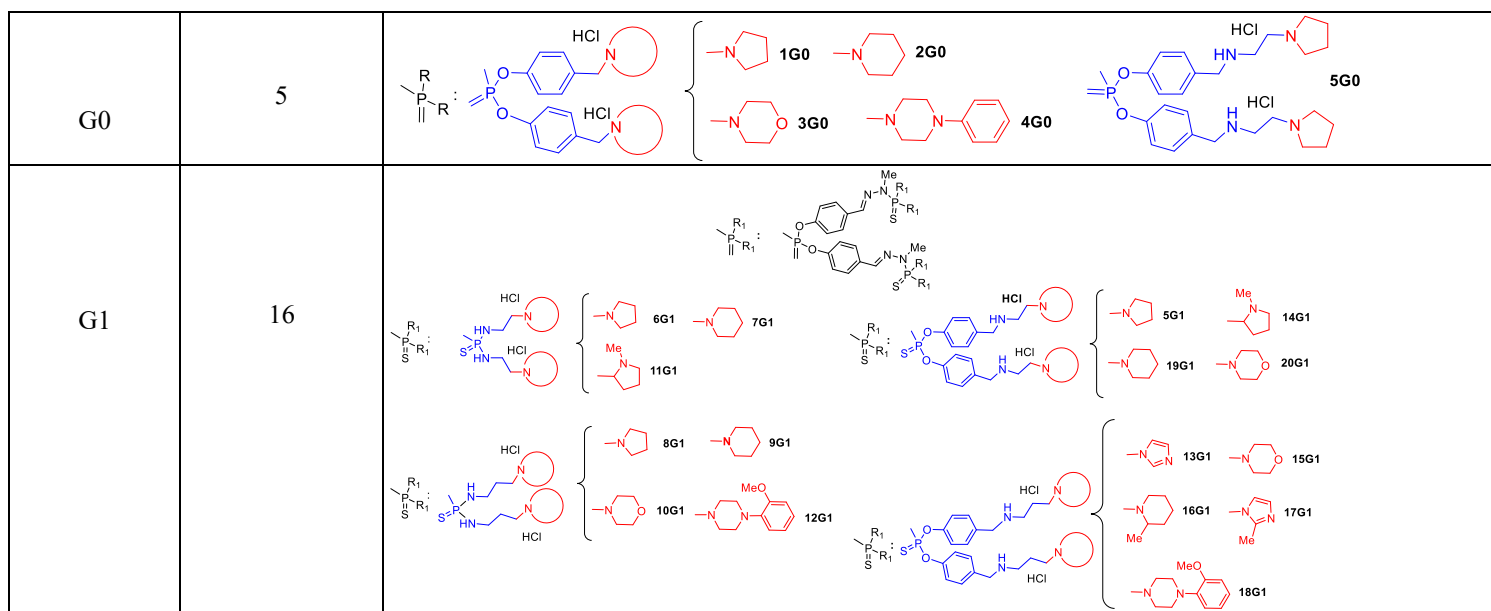


Scheme 4. General synthesis of dendrimers **6G2,HCl**, **7G2,HCl**, **6G3,HCl**, **7G3,HCl**, **6G4,HCl** and **7G4,HCl**.

As shown in the Schemes 1-3, firstly, we have prepared a library of dendrimers generation 0 (6 amino groups on the surface) and generation 1 (12 amino groups on the surface) containing 5 and 16 functionalized dendrimers, respectively (Table 1). These dendrimers have on their surface diverse types of amino groups such as pyrrolidinium, *N*-methyl pyrrolidinium, piperidinium, *N*-methyl piperidinium, morpholinium, imidazolium, 2-methyl-imidazolium, 1-phenyl-piperazinium, and (2-methoxy)-1-phenyl-piperazinium. As shown in Table 1, several linker types have been introduced between the cyclotriphosphazene core ring and the diverse amino groups on the surface.

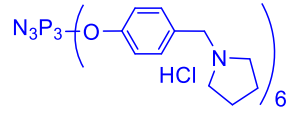
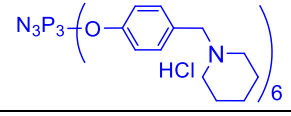
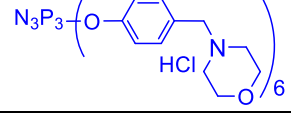
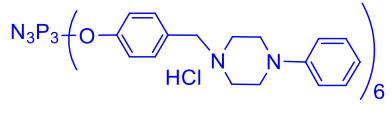
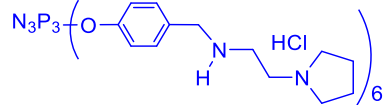
Table 1. Chemical moieties on the surface of dendrimers of the generation 0 and 1 and from the last phosphorus atom on the considered branch.

Generation	Number of dendrimers prepared	Chemical moieties on the surface from the last phosphorus atom on the considered branch



Then, based on the very interesting anti-TB activities of the protonated form of dendrimers **1G0**, **2G0**, **6G1**, **7G1**, **9G1**, **11G1** and **20G1** (Tables 2 and 3), we decided to extend the structure-activity relationships to the construction of libraries of generation 2 (G2, Table 4), 3 (G3, Table 5) and 4 (G4, Table 6) incorporating 2 phosphorus dendrimer types each. These phosphorus dendrimers have protonated pyrrolidino and piperidino moieties, which showed good anti TB activities with dendrimers of generation 0 and 1 (Table 2 and 3). Generation 2 and 3 are decorated on their surface with 24 or 48 protonated pyrrolidino or piperidino groups while 96 pyrrolidinium and piperidinium groups are grafted on the surface of a dendrimer of generation 4.

Table 2: Antitubercular activity of generation zero dendrimers

S. No.	Number of amino groups on the surface	Chemical Structure	CC ₅₀ (Vero Cell line) (µg/ml)	Anti-mycobacterial Activity* (µg/ml)			Intracellular Activity* J774A.1 (µg/ml)	
				<i>MTB</i> H37Ra	<i>M. bovis</i> BCG	<i>MTB</i> H37Rv	<i>MTB</i> H37Ra	<i>MTB</i> H37 Rv
1G_{0,HCl}	6		10	12.5	12.5	3.12	Inactive	Not done
2G_{0,HCl}	6		50	25	25	3.12	12.5	6.12
3G_{0,HCl}	6		100	Inactive	Inactive	6.25	Inactive	Inactive
4G_{0,HCl}	6		50	Inactive	Inactive	Inactive	Inactive	Not done
5G_{0,HCl}	6		25	50	100	Inactive	Inactive	Not done

*The two-fold dilutions of each compound were screened. The experiments were repeated three times

Table 3: Antitubercular activity of generation one dendrimers

S. No.	Number of amino groups on the surface	Chemical Structure	CC ₅₀ (Vero Cell line) (µg/ml)	Anti-mycobacterial Activity* (µg/ml)			Intracellular Activity* J774A.1 (µg/ml)	
				MTB H37Ra	<i>M. bovis</i> BCG	MTB H37Rv	MTB H37Ra	MT BH3 7 Rv
6G1,HCl	12		40	25	12.5	Inactive	Inactive	Not done
7G1,HCl	12		40	25	12.5	Inactive	Inactive	Not done
8G1,HCl	12		25	50	Inactive	Inactive	Inactive	Not done
9G1,HCl	12		25	25	25	Inactive	Inactive	Not done

10G1,HCl	12		100	100	Inactive	Inactive	Inactive	Not done
11G1,HCl	12		50	25	25	Inactive	Inactive	Not done
12G1,HCl	12		50	Inactive	Inactive	Inactive	Inactive	Not done
5G1,HCl	12		200	50	Inactive	Inactive	Inactive	Not done
13G1,HCl	12		100	100	Inactive	Inactive	Inactive	Not done
14G1,HCl	12		50	Inactive	Inactive	Inactive	Inactive	Not done
15G1,HCl	12		50	Inactive	Inactive	Inactive	Inactive	Not done
16G1,HCl	12		25	50	25	Inactive	Inactive	Not done

17G1,HCl	12		50	50	25	Inactive	Inactive	Not done
18G1,HCl	12		50	Inactive	Inactive	Inactive	Inactive	Not done
19G1,HCl	12		100	100	100	Inactive	Inactive	Not done
20G1,HCl	12		100	25	25	Inactive	Inactive	Not done

*The two-fold dilutions of each compound were screened. The experiments were repeated three times

Table 4: Antitubercular activity of generation two dendrimers

S. No.	Number of amino groups on the surface	Chemical Structure 	CC ₅₀ (Vero Cell line) (µg/ml)	Anti-mycobacterial Activity* (µg/ml)			Intracellular Activity* J774A.1 (µg/ml)	
				MTB H37Ra	M. bovis BCG	MTB H37Rv	MTB H37Ra	MTBH37 Rv
6G2,HCl	24		40	50	Inactive	Inactive	Inactive	Not done
7G2,HCl	24		640	Inactive	Inactive	Inactive	Inactive	Not done

*The two-fold dilutions of each compound were screened. The experiments were repeated three times

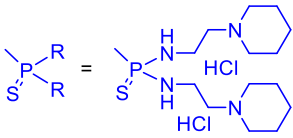
Table 5: Antitubercular activity of generation three dendrimers

S. No.	Number of amino groups on the surface	Chemical structure 	CC50 (vero cell line) (µg/ml)	Antimycobacterial activity*(µg/ml)			Intracellular activity-J774A.1* (µg/ml)
				<i>M. tub.</i> H37Ra	<i>M. bovis</i> BCG	<i>M. tub.</i> H37Rv	
6G3,HCl	48		>160	>100	>100	>25	>6.25
7G3,HCl	48		>640	>100	>100	>25	>6.25

*The two-fold dilutions of each compound were screened. The experiments were repeated three times

Table 6: Antitubercular activity of generation four dendrimers

S. No.	Number of amino groups on the surface	Chemical structure 	CC50 (vero cell line) (µg/ml)	Antimycobacterial activity* (µg/ml)			Intracellular activity-J774A.1* (µg/ml)
				<i>M. tub.</i> H37Ra	<i>M. bovis</i> BCG	<i>M. tub.</i> H37Rv	
6G4,HCl	96		<50	>100	>100	>6.25	>6.25

7G4 _{HCl}	96		>100	>100	>100	>6.25	>6.25
--------------------	----	---	------	------	------	-------	-------

*The two-fold dilutions of each compound were screened. The experiments were repeated three times

RESULTS AND DISCUSSION

We decided to develop a phenotypic screening strategy, in contrast to the target-based strategy, although the latter has been widely used in drug discovery since the molecular biology revolution of the 1980s.³⁴ Indeed, the main advantages of phenotypic screens are as follows: 1) design and construction of pre-selected compound collections with drug-like properties and optimizable chemical features to monitor efficacy and druggability, in our case construction of a biocompatible and tunable phosphorus dendrimer collection within the dendrimer space;^{35, 36} 2) powerful assay development such as affinity, cellular profiling, and functional genomics-based approaches to screen the collections; 3) elucidation of the target(s) related to the mechanism of action by several powerful well-known technologies;³⁸ 4) elucidation of off-targets based on unwanted secondary phenotypes, and 5) high attrition rate in the anti-infective drug discovery,³⁷ and 6) limited validated targets in the TB field.²⁶

Molecular modeling studies

Conformational space, surface properties, and molecular dynamics of three-dimensional all-atom models of **1G0_{HCl}** and **2G0_{HCl}** of the developed phosphorous dendrimer library were explored by classical force field methods. Conformational searches identified the low potential energy conformations depicted in Figure 2. Both, fully protonated **1G0** and **2G0** present a solvent-accessible surface area (SASA) with very dominantly positive or neutral potential energy arising to over 85% from the branches. Very localized spots of less than 15% of the entire surface have a negative potential energy arising from solvent exposed regions of the N₃P₃ core. Such surface patches give rise to hydrogen bonds formed by the core to water molecules steadily observed during molecular dynamics simulations.

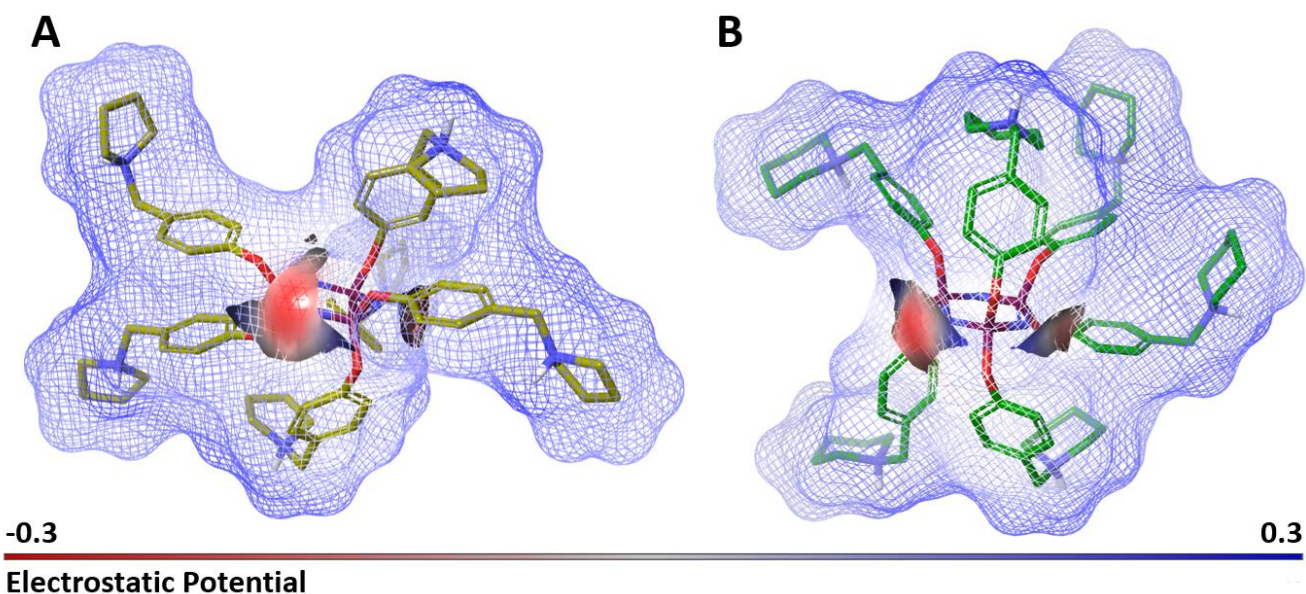


Figure 2. Three-dimensional models of fully protonated **1G0** (A) et **2G0** (B). The models are the lowest energy conformations issued from conformational searches applying an implicit solvent model. Solvent-accessible surface area (SASA) arising from the entire dendrimer or N_3P_3 core only are depicted as mesh or solid, respectively; colour ramp by potential energy from -0.3 in red over neutral in white to 0.3 in blue. The chemical structure of the dendrimers is depicted as tubes with carbon, oxygen, nitrogen, phosphor, and hydrogen atoms indicated in green shades, red, blue, purple, and white, respectively; nonpolar hydrogen atoms are not represented for clarity.

These molecular dynamics simulations of **1G0**_{HCl} and **2G0**_{HCl} in explicit aqueous solution evince irregularly shaped nanoparticles of changing form with a radius of gyration of roughly 7 Å (Supplements Figures 1 and 2), minimal and maximal dimensions of 14 to 15 Å and about 25 Å, respectively (Supplements Figures 3 and 4). The core typically maintains hydrogen bonds to 3 or 4 water molecules throughout the entire simulation (Supplements Figures 1 and 2). The protonated tertiary amines of the branches distribute rather evenly around the central N_3P_3 core (Figure 3) and their spatial distribution relative to each other is very similar for **1G0**_{HCl} and **2G0**_{HCl} (Supplements Figures 5 and 6). The nitrogen atoms tend to be at a distance of 7.5 Å when analyzing branches above or below the core and assuming conformations that extend roughly perpendicularly to the N_3P_3 plane (Supplements Figures 5A, 5B, 6A, and 6B). These conformations give rise to distances of about 14 Å when analyzing nitrogen atoms above the N_3P_3 plane with respect to those below (Supplements Figures 5C and 6C). Branch conformations that strongly tilt towards the N_3P_3 plane and approach nitrogen

atoms of branches above and below the plane, again give rise to nitrogen distances of about 7 Å (Supplements Figures 5C and 6C). Branch conformations are highly mobile switching frequently from perpendicular to tilted and back, thereby distributing the positively charged nitrogen atoms evenly around the core and optimizing the electrostatic repulsion between the charged groups. Furthermore, **1G0_{HCl}** and **2G0_{HCl}** show numerous intramolecular interactions or form hydrogen bonds and ion pairs with solvent molecules (Figure 3). Transitory ion pairs formed with chlorine include two branches simultaneously binding to one chlorine ion. Classical and aromatic hydrogen bonds to water, intramolecular parallel or perpendicular π -stacking, and intramolecular cation- π -interactions are also observed (Figure 3). Altogether **1G0_{HCl}** and **2G0_{HCl}** show very similar molecular dynamics and globally expose the same appearance to potentially interacting macromolecules of their biological environment.

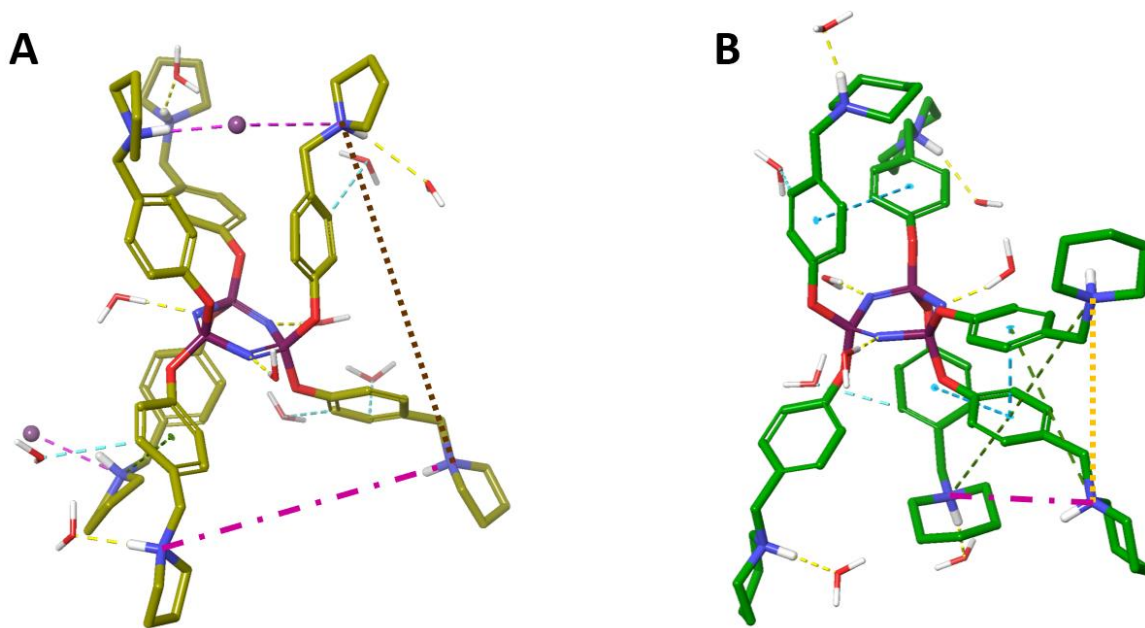


Figure 3. Snapshots of **1G0_{HCl}** and **2G0_{HCl}** from the molecular dynamics simulations in A and B, respectively. Classical and aromatic hydrogen bonds to water, ion pairs with chlorine, parallel or perpendicular π -stacking, and cation- π -interactions are indicated by dashed lines in yellow, light blue, magenta, cyan, and green, respectively. Dendrimer and water molecules are depicted in tube representation, chlorine ions as spheres colored in plum, otherwise color coding as in Figure 2; non-polar hydrogens not depicted for clarity. Dotted lines in orange or brown exemplarily highlight protonated tertiary amine distances giving rise to radial distribution function (rdf) maxima Max1 or

Max2, respectively, in Supplements Figures 5C and 6C; dash-dotted lines in magenta exemplarily indicate distances of rdf in Supplements Figures 5A/B and 6A/B.

***In vitro* activity of Phosphorous dendrimers and their cytotoxicity**

The entire phosphorus dendrimer collection was firstly tested for its antimycobacterial activity against three different strains such as attenuated and virulent *M. tuberculosis* H37Ra and H37Rv, respectively, as well as *Mycobacterium bovis* BCG. The toxicity of the phosphorus dendrimers was evaluated against Vero cell lines which were isolated from kidney epithelial cells extracted from African green monkey.

Within the generation 0 series, the antimycobacterial activities assessed as Minimum Inhibitory Concentration (MIC) against the three strains H37Ra, BCG, and H37Rv in order are: **1G_{0,HCl}** (MICs in µg/ml = 12.5 for Ra, 12.5 for BCG, and 3.12 for Rv), **2G_{0,HCl}** (MICs in µg/ml = 25.0 for Ra, 25.0 for BCG, and 3.12 for Rv), **3G_{0,HCl}** (MIC = 6.25 µg/ml against Rv) and **5G_{0,HCl}** (MICs in µg/ml = 50 for Ra and 100 for BCG) in extra-cellular killing of mycobacteria (Table 2). The dendrimer **4G_{0,HCl}** displayed no antimycobacterial activity. **1G_{0,HCl}** has pyrrolidinium groups on its surface, whereas **2G_{0,HCl}** has piperidinium groups with the same linker 4-(aminomethyl)phenoxy moiety. The replacement of the pyrrolidinium or the piperidinium group on the surface by either a morpholinium group (compound **3G_{0,HCl}**) or 4-phenyl piperidinium group (compound **4G_{0,HCl}**) decrease the antimycobacterial activities *versus* **1G_{0,HCl}** and **2G_{0,HCl}**. The increase of the chain length of **1G_{0,HCl}**, leading to dendrimer **5G_{0,HCl}** with the 4-((2-aminoethyl)amino)methyl)phenoxy chain, decreased also the antimycobacterial activities against the three strains. Interestingly, the safety index SI defined as CC₅₀ against Vero cell line divided by MICs is 16.02 *versus* Ra and 3.1 *versus* Ra for **2G_{0,HCl}** and **1G_{0,HCl}**, respectively. Very interestingly, as shown in Table 7, when activity of **2G_{0,HCl}** and **3G_{0,HCl}** were tested against SDR *M.tuberculosis*, **2G_{0,HCl}** was found to be active against all the SDR strains whereas, **3G_{0,HCl}** demonstrated a moderate activity against Rifampicin, Isoniazid and Ethambutol resistant H37Rv but was inactive against Streptomycin resistant H37Rv. *Consequently, 2G_{0,HCl} represents a particularly interesting and safe anti-TB agent based on cellular assays.*

TABLE 7 2G0,HCl is active against all the single drug-resistant Mtb strains

S.No	Compound	<i>M. tuberculosis</i> H37Rv (µg/mL)	MTB strain resistant to			
			INH (µg/mL)	RIF (µg/mL)	ETB (µg/mL)	STR (µg/mL)
1	2G0,HCl	3.12	6.25	6.25	6.25	6.25
2	3G0,HCl	6.25	25	12.5	25	>64
3	Rifampicin	0.04	0.04	>64	0.19	0.04
4	Isoniazid	0.04	>64	0.04	0.04	0.04
5	Ethambutol	3.12	NT	NT	>64	0.78
6	Streptomycin	1.56	NT	NT	12.5	>64

*RIF: Rifampicin, INH: Isoniazid, ETB: Ethambutol, STR: Streptomycin, NT: Not Tested.

In order to establish additional structure-activity relationships (SARs) based on modification of generations, surface amino groups and branches, as highlighted in Table 2, we then decided to synthesize the next generation, G1 (12 amino groups on the surface), by introducing five different types of linkers (branches) between the dendrimer core and the different amino groups on the surface: *NH*-amino-ethyl-amine (**6G1,HCl**, **7G1,HCl** and **11G1,HCl**), *NH*-amino-propyl-amine (**8G1,HCl**-**10G1,HCl** and **12G1,HCl**), 4-(((2-aminoethyl)amino)methyl)phenoxy (**5G1,HCl**, **14G1,HCl**, and **19G1,HCl**-**20G1,HCl**), and 4-(((2-aminopropyl)amino)methyl)phenoxy (**13G1,HCl**, **15G1,HCl**-**18G1,HCl**). As a general remark, several observations are apparent. All the protonated forms of these 16 G1 dendrimers displayed lower potency against the three selected strains *versus* dendrimers of generation 0. Within the G1 series, the most interesting G1 dendrimers are again pyrrolidinium or piperidinium groups bearing **6G1,HCl** and **7G1,HCl**. However, they showed moderate antimycobacterial activities only against *MTB* H37Ra and *M. Bovis* BCG with MICs of 25 and 12.5 µg/ml, respectively, like those of **1G0,HCl**, **2G0,HCl** and **5G0,HCl**, and no activity against *MTB* H37Rv. The phosphorus dendrimers **6G1,HCl**, **7G1,HCl** and **5G0,HCl** have the same 2-(pyrrolidin-1-yl)ethanaminium group or 2-(piperidin-1-yl)ethanaminium group on the surface. The lengthening of the chain of **6G1,HCl** and **7G1,HCl** with the same amino group on the surface decreased antimycobacterial activities, **8G1,HCl** *versus* **6G1,HCl** and **9G1,HCl** *versus* **7G1,HCl** showing MICs of ~25-50µg/ml. The replacement of the piperidinium group of **9G1,HCl** by a morpholinium group (**10G1,HCl**) with the same linker did not improve potency, whereas the introduction of a 1-methylpyrrolidinium group substituted in position 2 (**11G1,HCl**) maintains the

moderate antimycobacterial activities only against *MTB* H37Ra and *M. Bovis* BCG with MICs of 25 µg/ml. No activity has been observed by the introduction of (2-methoxy)-1-phenyl-piperazinium group in place of pyrrolidinium or piperidinium groups (**12G1,HCl** versus **8G1,HCl** or **9G1,HCl**). The replacement of the *NH*-amino-ethyl-amine or the *NH*-amino-propyl-amine chains by the 4-(((2-aminoethyl)amino)methyl)phenoxy chain (**14G1,HCl**, **19G1,HCl**, and **20G1,HCl**) or by 4-(((3-aminopropyl)amino)methyl) phenoxy chain (**13G1,HCl**, and **18G1,HCl**) did not improve the antimycobacterial activities whatever the nature of the amino groups on the surface (pyrrolidinium (**6G1,HCl**), piperidinium (**19G1,HCl**), morpholinium (**20G1,HCl**, and **15G1,HCl**), imidazolium (**13G1,HCl** and **17G1,HCl**), 1-methylpyrrolidinium group substituted in position 2 (**14G1,HCl**), 2-methylpiperidinium (**16G1,HCl**), and (2-methoxy)-1-phenyl-piperazinium (**18G1,HCl**) groups). For generation 1, in contrast to generation 0, no effect of the nature of the amino groups on the surface has been clearly demonstrated. All the dendrimers showed moderate to no antimycobacterial activities. To summarize, the most relevant G1 dendrimers are **6G1,HCl** and **7G1,HCl** with the shorter chain (*NH*-amino-ethyl-amine) and the pyrrolidinium and piperidinium groups on the surface.

Based on the very interesting results for **1G0**, **2G0**, **6G1**, and **7G1**, we decided to construct a series of six dendrimers of generation 2, 3, and 4 bearing on the surface only the pyrrolidinium and piperidinium groups (Tables 4-6). The dendrimers **6G2,HCl** and **7G2,HCl**, **6G3,HCl** and **7G3,HCl**, and **6G4,HCl** and **7G4,HCl** showed no antimycobacterial activities against all three strains, except **6G2,HCl** showing poor anti-TB activities against only *MTB* H37Ra with MIC of 50 µg/ml but a SI of 0.8.

Interestingly, **2G0**, inhibited the mycobacterial growth and intracellular survival in infected J774 A.1 cells. **2G0,HCl** showed extracellular killing of *MTB* H37Rv with MICs of 6.12 µg/ml. In order to assure the effect of dendrimers on intracellular replicating mycobacteria, we have tested the dendrimers **2G0,HCl** and **3G0,HCl**. The effect of dendrimer **1G0,HCl** on intracellularly replicating bacteria was not done due to its low CC₅₀. For analysis of effect of dendrimers on intracellular bacteria, we infected J774A.1 cells with *MTB* H37Rv and treated with different concentrations of dendrimers ranging from 0.78 to 25 µg/ml. After 48 h post infection the cells were harvested and added to the intracellular bacteria on LJ slants from treated and untreated cells. As shown in Figure 4, after 4-5 weeks of incubation the colony-forming units (CFUs) were calculated and it was observed that the *MTB* infected cells treated with **2G0,HCl** showed no intracellular bacteria at the concentration above 6.25 µg/ml. The

dendrimer **3G0_{HCl}** exhibited marginal effect on intracellularly replicating MTB H37Rv. In these assays, Rifampicin was used as a positive control.

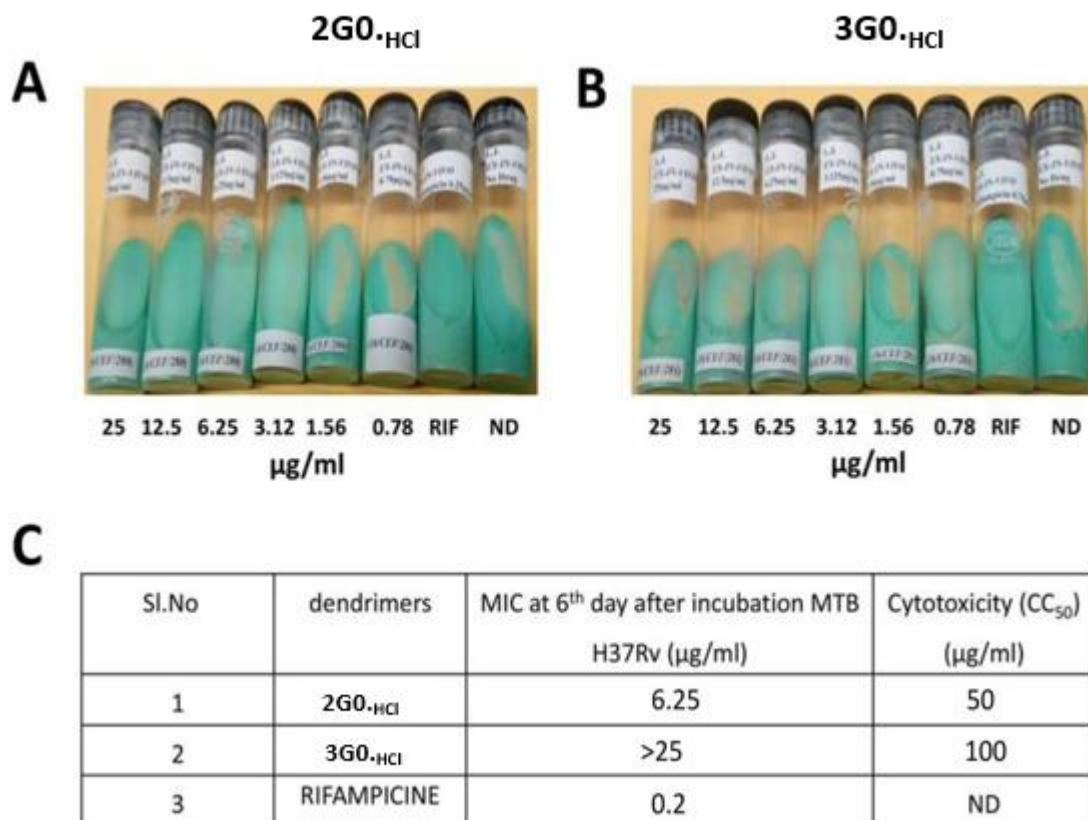


Figure 4. Intracellular activity of Dendrimers against infected macrophages. LJ slants showing the growth of bacteria in presence of dendrimer **2G0_{HCl}** (A) and dendrimer **3G0_{HCl}** (B) *versus* Rifampicin (RIF), ND: no drug. Table (C) showing the MICs and CC_{50s} of both the dendrimers.

Specificity of the active dendrimers

To determine its antimicrobial specificity, activity of **2G0_{HCl}** and **3G0_{HCl}** were also determined against an ESKAPE panel consisting of *Escherichia coli* ATCC 25922, *Staphylococcus aureus* ATCC 29213, *Klebsiella pneumoniae* BAA-1705, *Acinetobacter baumannii* BAA-1605 and *Pseudomonas aeruginosa* ATCC 27853 where both were found to be completely inactive indicating that its antimicrobial activity is *Mycobacterium sp.* specific.

As a general statement, the size of dendrimers as well as the nature of the terminal group play key roles. Dendrimers of generation 0 bearing pyrrolidinium or piperidinium groups displayed good antimycobacterial activities against the three selected strains. In this direction, moderate biological activities were observed with generation 1 only with the shorter chain and also with the pyrrolidinium and piperidinium groups on the surface. Figure 5 represents the principal SARs amongst the prepared dendrimers between the generation of dendrimers and the antimycobacterial activities.

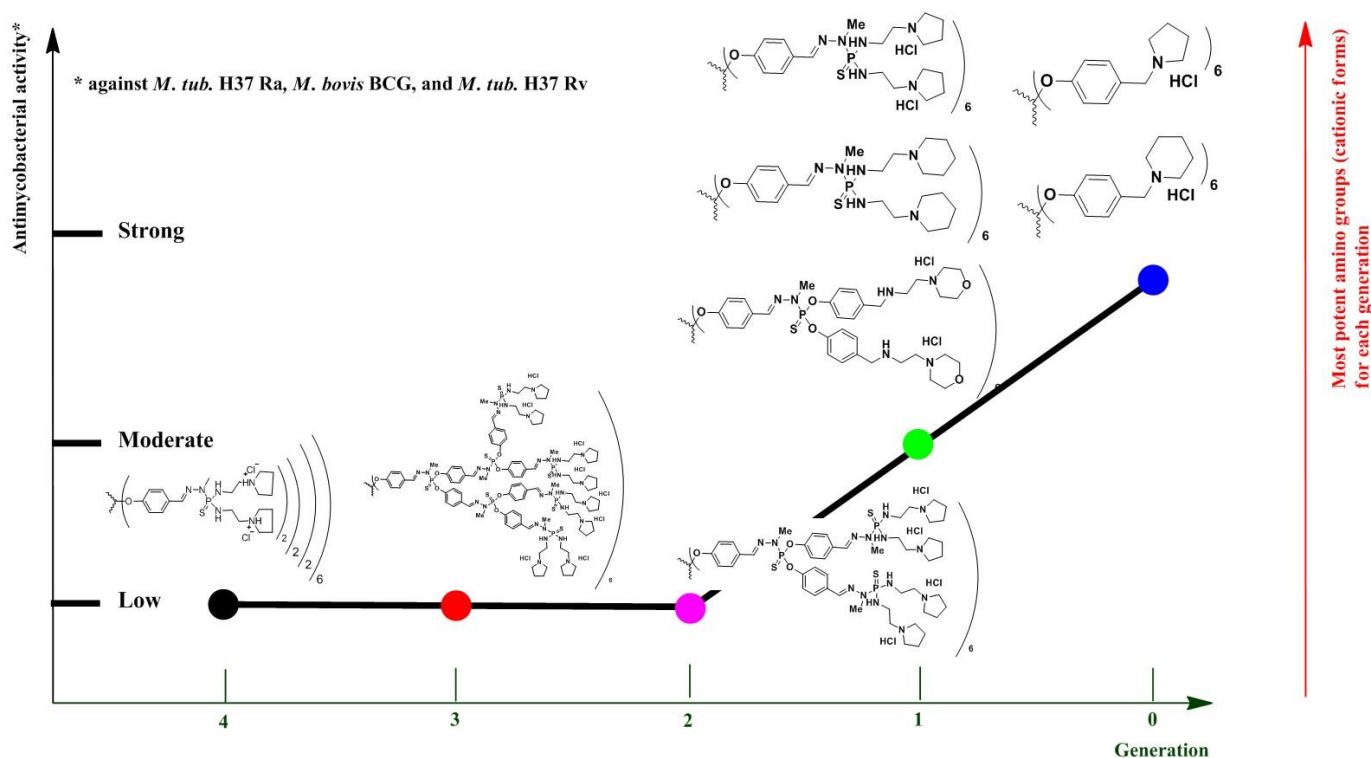


Figure 5. Main structure activity relationships between the generation of dendrimers and antimycobacterial activities.

Taken together, these results fully confirm the interest of **2G_{0,HCl}** as a safe antitubercular agent active against resistant strains. Consequently, **2G_{0,HCl}** was tested in an animal model through oral administration.

Efficacy of **2G_{0,HCl}** in Balb/C mice against MtbH37 Ra

Since **2G_{0,HCl}** demonstrated safe and potent *in vitro* antimycobacterial activity, we decided to evaluate its *in vivo* efficacy in Balb/C mice. Two weeks oral treatment with 33 mg/Kg of **2G_{0,HCl}** (one-time

daily administration) reduced the mean bacterial counts in lung of infected mice significantly by 1.0 log₁₀ while 50 mg/Kg of **2G0_{HCl}** reduced bacterial counts by ~1.5 log₁₀ as compared to the untreated group. This outcome is even better compared to Rifampicin treated groups. Taken together, this important experiment demonstrates the superior efficacy of **2G0_{HCl}** in clearing infection from various animal tissues in comparison to Ethambutol and Rifampicin (Figure 6).

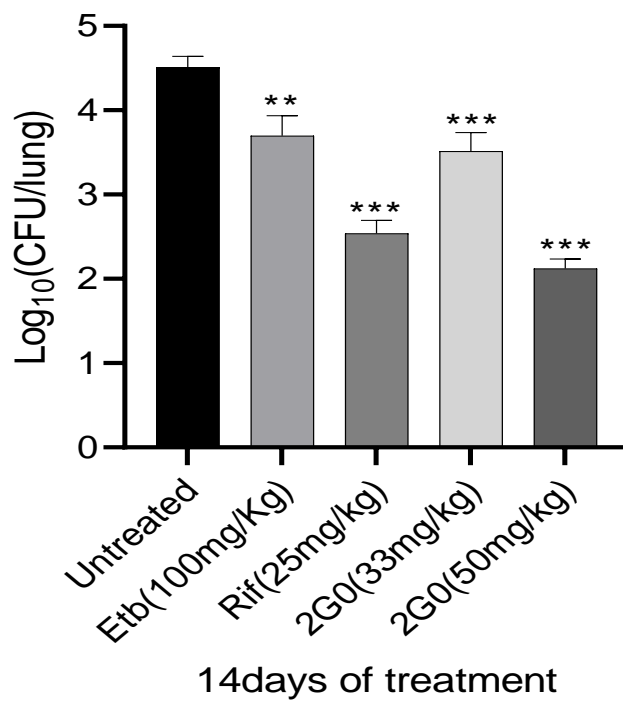


Figure 6: *In vivo* efficacy of **2G0_{HCl}** in Balb/C mice. Mean log₁₀ CFU/ml in lungs of mice after 14 days post-treatment with **2G0_{HCl}** (oral administration, once daily during two weeks), Rifampicin and Ethambutol. Mice were infected intravenously with ~10⁶ CFU of *M. tuberculosis* H37Rv and treatment was started 7 days post infection.

Mechanism of action studies of 2G0_{HCl}: First investigations

Since **2G0_{HCl}**, demonstrated good *in vitro*, *ex vivo*, and *in vivo* activities, it was imperative to elucidate the mechanism of action by which killing of *MTB* H37Rv is facilitated. MALDI MS-MS data showed differential regulation of 15 specific proteins which have been shown in Table 8 and Figure 7.

Within the 15 proteins observed, three were upregulated as there are SodA (Fe), Unnamed Gi15607825 Rv0685 and Elongation factor TU Rv0685. Another twelve were downregulated as there are GAPDH Rv1436, Alkyl hydroperoxidasereductase subunit-c Rv2428, DnaK Rv0350, Hypothetical protein Rv0020c, Rv 2145c, Phosphopyruvatehydratage, DNA directed RNA polymerase alpha subunit, Malate dehydrogenase, Flavoprotein alpha subunit, and Two component response regulator protein MprA. Detailed functional characterization of differentially expressed proteins is required to identify the exact mechanism of action of the dendrimers.

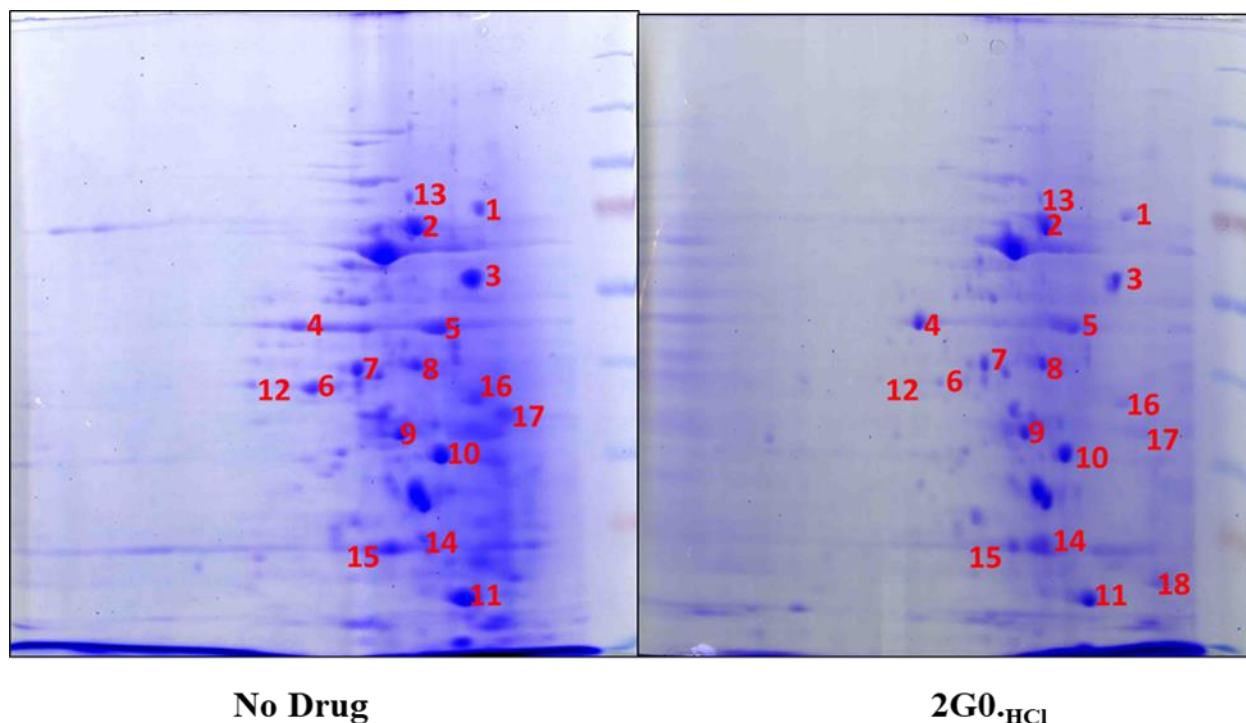


Figure 7: 2D gel profile of *MTB* H37Ra treated with **2G0_{HCl}**

TABLE 8: List of MTB proteins and their functions

Identified Proteins	Expression level of proteins	Role in MTB
SodA (Fe)	Upregulation	TB leads to increased oxidative burden (ROS, RNI) in the lung that aids in the activation of TB prodrugs. SodA (Fe) destroys radicals which are normally produced within the cells and are toxic to biological systems ($O_2^- \rightarrow H_2O_2$)
Unnamed Gi15607825 Rv0685	Upregulation	Promotes GTP-dependent binding of aminoacyl-tRNA to the A-site of ribosomes during protein biosynthesis.
Elongation factor TU Rv0685	Upregulation	Promotes GTP-dependent binding of aminoacyl-tRNA to the A-site of ribosomes during protein biosynthesis.
GAPDH Rv1436	Downregulation	Involved in second phase of glycolysis
Alkyl hydroperoxidasereductase subunit-c Rv2428	Downregulation	Involved in oxidative stress response
DnaK Rv0350	Downregulation	Acts as a chaperone. Involved in induction by stress conditions e.g. heat shock. Possibly has an ATPase activity
Hypothetical protein Rv0020c	Downregulation	Signal transduction
Rv 2145c	Downregulation	Cell division
Phosphopyruvatehydratase	Downregulation	Anchorless surface exposed proteins that binds to plasminogen
DNA directed RNA polymerase alpha subunit	Downregulation	DNA-dependent RNA polymerase catalyzes the transcription of DNA into RNA

Malate dehydrogenase	Downregulation	Involved in the conversion of malate to oxaloacetate
Flavoprotein alpha subunit	Downregulation	The electron transfer flavoprotein serves as a specific electron acceptor for other dehydrogenases
Two component response regulator protein MprA	Downregulation	Regulator, part of a two component regulatory system

Furthermore and importantly, **2G0,HCl** is stable at room temperature in aerated aqueous solution at pH 5.5 to 6 for at least 9 months without any chemical degradation. This point is very important *for in vivo* experiments (*vide infra*) and potential clinical development.^{38, 39}

CONCLUSION AND PERSPECTIVES

TB is an old infectious disease mainly affecting the lungs caused by *Mycobacterium tuberculosis*. Compared with other diseases, TB is one of the most important killers, and TB medication can be toxic to the liver. In addition, most of the TB drugs are, in fact, bio precursor-type prodrugs.⁴⁰ Development of MDR- and XDR-TB warrants the introduction of new chemotherapeutic tools in the arsenal of anti-TB drugs. Consequently, the search of original anti-TB derivatives with a broad spectrum and with a new scaffold is even more pertinent today. Very interestingly, we developed original anti-TB compounds based on biocompatible polycationic phosphorus dendrimers. These nanoparticles open new avenues in the tuberculosis domain and are chemically totally different from and not related to the standard anti-TB drugs. The most potent dendrimers have a very simple structure: generation 0 bearing 6 groups on their surface, either pyrrolidinium groups (**1G0,HCl**) or piperidinium groups (**2G0,HCl**). They are irregularly shaped dendrimers of changing form due to highly mobile branches. Their radius of gyration is roughly 7 Å, minimal and maximal diameters are 14 to 15 Å and 25 Å, respectively. Their SASA is dominantly positive due to the rather evenly distributed protonated tertiary amines with localized negative spots arising from the central N₃P₃ ring. The protonated amines form transient ion pairs with chlorine in MD simulations, whilst the central core typically interacts with three to four water molecules. Altogether they present a very similar appearance to macromolecules of their biological environment. **1G0,HCl** and **2G0,HCl** are active against three different strains such as attenuated *M. tuberculosis H37Ra*, virulent *M. tuberculosis H37Rv* as well as against *Mycobacterium bovis BCG*.

Importantly, the safety index is 16.02 and 3.1 *versus* Ra for **2G0_{HCl}** and **1G0_{HCl}**, respectively. Very interestingly **2G0_{HCl}** was tested against single drug resistant *M.tuberculosis*, multiple strains resistant to Rifampicin, Isoniazid, Ethambutol, or Streptomycin. **2G0_{HCl}** showed activity against all single drug resistant strains which indicates that the dendrimers possess a potential new mode of action. Moreover, our preliminary studies on their mechanism of action suggested that **2G0_{HCl}** acts on novel targets and/or pathways. In addition, **2G0_{HCl}** inhibited the mycobacterial growth and intracellular survival in infected J774 A.1 cells. Consequently, **2G0_{HCl}** represents a very interesting and safe anti-TB agent and was selected for *in vivo* experiments. A single daily oral administration for a fortnight with 50 mg/Kg of **2G0_{HCl}** very significantly reduces the mean bacterial count in the lungs of infected mice by about 1.5 log₁₀ compared to the untreated group. This bacterial reduction is greater than that observed in the Rifampicin and Ethambutol treated groups.

Taken together, all of the *in vitro*, *in cellular*, *ex vivo*, and *in vivo* experiments demonstrated that the safe and chemically stable, G0 polycationic phosphorus dendrimer named **2G0_{HCl}** represents a new chemical entity to tackle tuberculosis. Moreover, **2G0_{HCl}** is up to 9 months in aerated aqueous solution chemically stable, which is one of the critical points for potential clinical development. Interestingly, these original phosphorus dendrimers should be developed in combination therapy (multidrug regimens) to treat TB, for instance with Isoniazid, Rifampicin, or Delamanid which are currently used. The objective is to increase treatment efficacy while avoiding resistance (MDR-TB and XDR-TB). We are convinced that the main goals concerning the development of new TB drugs are to: 1) reduce the duration of treatment; 2) effectively treat MDR-TB; and, 3) provide treatment for patients with latent TB infection. Our original results may open new perspectives in these challenging fields.

METHODS SECTION

Molecular modeling

Molecular modeling employed the Drug Discovery Suite release 2020.u2 commercialized by Schrödinger Inc executed on a linux workstation with CentOS7 operating system. Three-dimensional all-atom models were constructed manually in graphical interface Maestro, energy optimized or minimized to convergence by programs Jaguar or Macromodel.^{41,42} Conformational searches and molecular dynamics (MD) simulations were conducted by programs Macromodel and Desmond, respectively.⁴³ Molecular mechanics (MM) all-atom molecular force field OPLS3 with implicit

aqueous solvent and standard settings were applied unless indicated otherwise.⁴⁴ In more detail, special care was taken to construct correct geometry of the N₃P₃ core as OPLS3 did not yield a planar conformation by MM energy minimization: cyclic (NP(OH)₂)₃ was quantum-mechanically energy optimized to convergence *in vacuo* by density functional theory (DFT) at the level of B3LYP-D3 theory applying basis set 6-31G, ** polarization, ++ diffuse basis functions, and no symmetry. Fully protonated models of **1G0** and **2G0** were derived from the optimized N₃P₃ core, the geometry of which was subsequently frozen in MM energy minimization, conformational searches, and MD simulations. Low-Frequency-Mode conformational searches of all rotatable, non-cyclic bonds were executed for 1000 steps, minimizing every conformer for 2500 steps maximum which only exceptionally did not yield converged geometry. The lowest energy conformers of fully protonated **1G0** and **2G0** served to calculate solvent-accessible surfaces and their properties as well as to setup MD simulations using the explicit SPC water model at pH 7, 0.154 M NaCl, and neutralizing the system by chlorine ions. Box margins of 20 Å in all three dimensions with optimized box orientation were applied. MD simulations were prepared and submitted via graphical interface Maestro. Simulations on NVIDIA V100 graphical processing units (GPUs) for 1 μs as NPT ensembles at 300K and 1atm constraining the N₃P₃ core by weight 300, employed infinite boundary conditions, Nose-Hoover chain thermostat, and Martyna-Tobias-Klein barostat after standard pre-equilibration. Energy values and atomic coordinates were recorded every 25 ps and 250 ps, respectively. Trajectories were analyzed interactively *via* Maestro by calculating Simulation Interaction Diagrams, hydrogen bonds of core or branches with water molecules, radii of gyration, and radial distribution functions. Standard quality analysis showed stable simulations in terms of potential and total energy, volume, temperature, and pressure. 1 μs simulation time sampled the conformational space well as deduced from the similar torsional distributions of equivalent rotatable bonds of the branches.

Bacterial strains, cell lines, growth conditions and animals

M. tuberculosis H37Ra, *M. tuberculosis* H37Rv and *M. Bovis* BCG were collected from American type culture collection (ATCC). Culture were grown in middlebrook (MB7H9) medium supplemented with 0.2 % glycerol, 0.05% tween 80 and 10%ADC. Cultures were incubated at 37°C. The J774A.1 murine macrophage cell line and VERO cells were acquired from ATCC and cultured in RPMI-1640 medium containing 2 mM L-glutamine, 1 mM sodium pyruvate, 4.5 g/L glucose, 1.5 g/L sodium bicarbonate,

10mM HEPES, supplemented with 10% heat inactivated Fetal bovine serum (FBS) at 37°C and 5% CO₂.

ANTI-MYCOBACTERIAL ACTIVITY

Microplate Alamar blue assay (MABA):

For the experiments, we used 96-well microplate with flat bottom and a well grown MTB H37Ra and *M. Bovis* BCG cultures of mid-log phase (OD₆₀₀ = 0.5-0.6) either in Sauton's medium supplemented with 3.5% glycerol and tween 80 or in MB7H9 medium. Initially dendrimers dilutions were prepared according to their solubility and subsequent two-fold dilution was performed in 0.15 ml of suspension cultures in each well of microplate. Two control wells were prepared, one containing only suspension culture and other containing suspension culture plus drugs (rifampicin and streptomycin). Microplates were incubated at 37°C for 2 to 3 days. After 48hrs of incubation the 10% alamar blue dye solution (Resazurin 0.03%) was added to all the wells and microplates were re-incubated at 37°C for 2 to 4 hrs and fluorescence was measured by spectrophotometer range from 530 to 590 nm.

Mycobacteria growth indicator tube (MGIT) assay:

The BACTEC MGIT 960 instrument is a fully automated system that exploits the fluorescence of an oxygen sensor to detect growth of mycobacteria in culture. MGIT tube contains 7 ml of modified middlebrook 7H9 broth base with OADC enrichment and PANTA; a mixture of antibiotics. For this experiment, 500µl MTB H37Rv cultures of mid-log phase (OD₆₀₀ = 0.5-0.6) were added to each MGIT tube. To which dendrimers at various concentrations were added. The relative growth ratio between the drug-containing tube and drug-free growth control (GC) tube was determined by the system's software algorithm. The final interpretation and the susceptibility results were reported by the M960 instrument automatically. The drugs from the MGIT SIRE kit were used as a positive control.

Activity against drug resistant *M. tuberculosis* strains:

Activity of the dendrimers were determined using MABA assay against drug-susceptible *Mycobacterium tuberculosis* H37Rv ATCC 27294 (virulent tubercle bacillus), INH-resistant *Mycobacterium tuberculosis* ATCC 35822 (isoniazid-resistant), RIF-resistant *Mycobacterium tuberculosis* ATCC 35838 (rifapicin-resistant), STR-resistant *Mycobacterium tuberculosis* ATCC

35820 (streptomycin-resistant), ETB-resistant *Mycobacterium tuberculosis* ATCC 35837 (ethambutol-resistant).

CYTOTOXICITY ASSAYS

For cytotoxicity assay, Vero cells (African green monkey kidney cell line) were added to 96-well plate at a concentration of 4×10^5 cells/well in complete RPMI medium. Vero cells were treated with dendrimers at different concentrations (10- to 12-fold of MIC) and were incubated at 37°C with 5% CO₂ for 24 hours to determine the response of dendrimers activity on cells. Two control wells; one containing only suspension culture as negative control and other containing suspension culture with ethanol as positive control were used. After 24 hrs of incubation the 10% alamar blue dye solution (Resazurin 0.03%) was added to all the suspension wells and microplates were re-incubated at 37°C for 2 to 4 hrs and florescence was measured at 530/590 nm.

Inhibition of Mycobacterial Growth and Survival in Infected J774 A.1 Cells:

The J774A.1 murine macrophage cell lines were maintained as described previously. For infection, the J774A.1 cell were seeded at the density of 5×10^4 cells/well in 24 well tissue culture plates. The log phase mycobacterial cultures were harvested by centrifugation at 2000x g for 10 minutes and washed for two times with sterile PBS and finally suspended in the RPMI-1640 medium. Prepared bacterial culture added in macrophages at 1:10 MOI, allowed for phagocytosis for 4 hours at 37°C and 5% CO₂. After 4 hours of phagocytosis, the medium was removed and washed twice with incomplete RPMI 1640 medium and supplemented with 100ug/ml amikacin for 2 hours for killing of extracellular mycobacteria. After 2 hours of amikacin treatment the medium was removed and washed twice with incomplete RPMI 1640 medium. The mycobacteria H37Rv infected J774A.1 cells were treated with dendrimers at different concentrations and cells were incubated at 37°C with 5% CO₂ for 48 hours to determine the response of dendrimers activity on intracellular bacteria. After 48 hours of dendrimers treatment, the medium was removed, and cells were washed twice with sterile PBS and finally 0.05% SDS was added to lyse the cells to release the bacteria. The intracellular bacteria were calculated by BACTEC MGIT 960 systems for the detection and recovery of mycobacteria by adding 0.1 ml of harvested MTB H37Ra suspension in MGIT tubes and allow reading tubes bar code trough BACTEC MGIT 960 system. The tubes were monitored each day for the fluorescence.

ANIMAL EXPERIMENTS

Animal experiments were performed on six-week-old BALB/c mice procured from National Laboratory Animal Facility, CSIR-CDRI. The experimental protocols were approved by the Institutional Animal Ethics Committee.

Determination of maximum tolerated dose and toxicity of dendrimers **2G0_{HCl}** in mice:

Based on high antitubercular activities of prepared dendrimers (Tables 2-6), the most efficient compound, **2G0_{HCl}**, was selected for *in vivo* experiments. Balb/c mice (6-7 weeks) of 20g weight were taken and were divided in 3 groups based on the given dose of 18/CEF/280 in mice. The oral dose set (in water) for the experiment was 50 mg/kg for the first group, 33mg/kg for the second group and no drug in the third group respectively. Route for the administration of the drug was kept oral and the mice were examined daily. All the animals in each group survived up to 3 months (100% survival after one-time daily administration during two weeks) and then were euthanized. In every day examination, we found that all the mice of group one and group two showed weight loss (approximately between 2-4 gm) of muscles mass and their behavior was found to aggressive (data not shown).

Efficacy of **2G0_{HCl}** in Balb/C mice against MtbH37 Ra

To determine the colony forming units in lungs of infected (with MtbH37Ra) Balb/C mice, we used 5 groups (No drug, **2G0_{HCl}** with 33mg/kg, **2G0_{HCl}** 50 mg/kg, Rifampicin 10 mg/kg and Ethambutol 100mg/kg) of Balb/C mice.

Female BALB/c mice 5 to 6 weeks old were taken for the experiment. The mice were divided into five groups (n=5). All groups were injected with MTB H37Ra intravenously. Animals were treated orally starting from seven days post infection daily for two weeks. After two weeks, all the mice were sacrificed, lung and spleen were homogenized in 5 mL normal saline, serially diluted and plated on Middlebrook 7H11 agar plates supplemented with OADC for bacillary load detection. After incubation for 4 weeks at 37°C, CFU were enumerated and the data was averaged across experiments.

Statistical analysis

Statistical analysis was performed using GraphPad Prism 6.0 software (GraphPad Software, La Jolla, CA, USA). Comparison between three or more groups was analyzed using one-way ANOVA, with post-hoc Tukey's multiple comparisons test. P-values of <0.05 were considered to be significant.

PRELIMINARY MECHANISM OF ACTION STUDIES OF 2G0_{HCl}

For this, sub lethal concentration of **2G0_{HCl}** (1.56 µg/ml) was used to treat MTB H37Ra for 2h. The equal amounts of whole MTB cells lysate proteins were separated by 1-DE, followed by 2-DE on 12% SDS-PAGE and stained with the Coomassie Brilliant Blue R-250. Stained Spots were cut out from the gels to process for MALDI MS-MS using standard gel digestion method with trypsin. Differently expressed Proteins were identified

Corresponding Authors

Jean-Pierre Majoral: jean-pierre.majoral@lcc-toulouse.fr; orcid.org/ 0000-0002-0971-817X

Serge Mignani: serge.mignani@paris and serge.mignani@staff.uma.pt; orcid.org/0000-0002-1383-5256

Arunava Dasgupta: a.dasgupta@cdri.res.in; orcid.org/0000-0001-9014-1904

Kishore K Srivastava: kishore@cdri.res.in; orcid.org/0000-0002-8225-229X

Rama P Tripathi: rpt.cdri@gmail.com; orcid.org/0000-0002-9256-3112

Authors

Anke Steinmetz; orcid.org/0000-0002-0856-4295

Anne-Marie Caminade; orcid.org/0000-0001-8487-3578

Swetarka Das; orcid.org/0000-0001-5305-844X

Shriya Singh; orcid.org/0000-0003-0397-5498

Author Contributions

All the other co-authors contributed equally.

Notes

The authors declare the following competing financial interest(s): A.S. is a Sanofi employee and may hold shares and/or stock options in the company.

ACKNOWLEDGEMENTS

We thank Director CSIR-CDRI for the support. Mignani S acknowledges the support of FCT-Fundacao para a Ciencia e a Tecnologia (project PEst-OE/QUI/UI0674/2013, CQM, Portuguese Government funds), and ARDITI through the project M1420-01-0145-FEDER-000005 - Centro de Quimica da Madeira - CQM+ (Madeira 14-20), and Majoral J-P, Caminade A-M Laurent R. and Karpus A. acknowledge the funds from Centre National de la Recherche Scientifique (CNRS, France). The work has been funded through Indo-French (CEFIPRA) project: CEFIPRA-5303-2.

SUPPORTING INFORMATION

Preparation and characterization of compounds of generation 0: 1G0, 2G0, 3G0, 5G0 and 1G0,HCl, 2G0,HCl, 3G0,HCl, 5G0,HCl; generation 1: 5G1, 6G1, 7G1, 8G1, 9G1, 10G1, 11G1, 12G1, 13G1, 14G1, 15G1, 17G1, 18G1, 19G, 20G1, 5G1,HCl, 6G1,HCl, 7G1,HCl, 8G1,HCl, 9G1,HCl, 10G1,HCl, 11G1,HCl, 12G1,HCl, 13G1,HCl, 14G1,HCl, 15G1,HCl, 17G1,HCl, 18G1,HCl, 19G1,HCl and 20G1,HCl.

Figures and statistics of non-covalent interaction counts, radii of gyration, and radial distribution functions observed by molecular dynamics simulations of 1G0,HCl and 2G0,HCl.

REFERENCES

1. Global tuberculosis report: World Health Organization, G. S., <https://apps.who.int/iris/bitstream/handle/10665/336069/9789240013131-eng.pdf>. 2020, (accessed January 2021).
2. Kendall, E. A.; Azman, A. S.; Cobelens, F. G., MDR-TB treatment as prevention: The projected population-level impact of expanded treatment for multidrug-resistant tuberculosis. . *PLoS One* **2017**, *12*, e0172748.

3. Moodley, R.; Godec, T. R.; STREAM, o. b. o. t., Trial Team. Short-course treatment for multidrug-resistant tuberculosis: the STREAM trials. *Eur. Respir. Rev.* **2016**, *25* (20), 29–35.
4. Gelperina, S.; Kisich, K.; Iseman, M. D.; Heifets, L., The Potential advantages of nanoparticle drug delivery systems in chemotherapy of tuberculosis. *Am. J. Respir. Crit. Care Med.* **2005**, *172*, 1487-1490.
5. Jawahar, N.; Reddy, G., Nanoparticles: A novel pulmonary drug delivery system for tuberculosis. *J. Pharm. Sci. & Res.* **2012**, *4*, 1901-1906.
6. Mignani, S.; Rodrigues, J.; Tomas, H.; Roy, R.; Shi, X.; Majoral, J.-P., Bench-to-bedside translation of dendrimers: Reality or utopia? A concise analysis. *Adv Drug Deliv Rev* **2018**, *136-137*, 73-81.
7. Arrowsmith, J., Trial watch: Phase II failures: 2008–2010. *Nat. Rev. Drug Discov.* **2011**, *10*, 328–329.
8. Hay, M.; Thomas, D. W.; Craighead, J. L.; Economides, C.; Rosenthal, J., Clinical development success rates for investigational drugs. *Nat. Biotechnol.* **2014**, *32*, 40–51.
9. Costa-Gouveia, J.; Amsa, J. A.; Brodin, P.; Lucia, A., How can nanoparticles contribute to antituberculosis therapy?. *Drug Discovery Today* **2017**, *22*, 600-607.
10. Pati, K.; Bagade, S.; Bonde, S.; Sharma, S.; Saraogi, G., Recent therapeutic approaches for the management of tuberculosis: Challenges and opportunities. *Biomedicine & Pharmacotherapy* **2018**, *99*, 735–745.
11. Skwarecki, A. S.; Milewskib, S.; Schielmann, M.; Milewska, M. J., Antimicrobial molecular nanocarrier-drug conjugates. *Nanomedicine: Nanotechnology, Biology, and Medicine* **2016**, *12*, 2215-2240.
12. Dineshkumar, P.; Panneerselvam, T.; Selvaraj, K. K.; Kumar, P. V., Formulation of rifampicin loaded PEGylated 5.0G EDA-PAMAM dendrimers as effective long-duration release drug carriers. . *Current Drug Therapy* **2017**, *12*, 115-126.
13. Bellini, G. R.; Guimar, A. P.; Pacheco, M. A. C.; Dias, D. A.; Furtadoc, V. R.; de Alencastro, R. B.; Hortac, B. A. C., Association of the anti-tuberculosis drug rifampicin with PAMAM dendrimer. *Journal of Molecular Graphics and Modelling* **2015**, *2*, 1-31.
14. Kumar, P. V.; Asthana, A.; Dutta, T.; Jain, N. K., Intracellular macrophage uptake of rifampicin loaded mannosylated dendrimers. *Journal of Drug Targeting* **2006**, *14*, 546–556.
15. Singh, N.; Gautam, S. P.; Harjaskaran; Singh, L.; Dhiman, A.; Siddiqui, G.; Verma, A., Isoniazid loaded dendrimer based nano carriers for the delivery of anti-tuberculosis. *Indian Research Journal of Pharmacy and Science* **2016**, *3*, 519-529.
16. Mignani, S.; Tripathi, R. P.; Chen, L.; Caminade, A.-M.; Shi, X.; Majoral, J.-P., New ways to treat tuberculosis using dendrimers as nanocarriers. *Pharmaceutics* **2018**, *10*, 0105.
17. Chis, A. A.; Dobrea, C.; Morgovan, C.; Arseniu, A. M.; Rus, L. L.; Butuca, A.; Juncan , A. M.; Totan, M.; Vonica-Tincu, A. L.; Cormos, G.; Muntean, A. C.; Muresan, M. L.; Gligor, F. G.; Frum, A., Applications and Limitations of Dendrimers in Biomedicine. *Molecules* **2020**, *25*, 3982.
18. Madaan, K.; Kumar, S.; Poonia, N.; Lather, V.; Pandita, D., Dendrimers in drug delivery and targeting: drug-dendrimer interactions and toxicity issues. *J. Pharm. Bioallied Sci.* **2014**, *6*, 139–150.
19. Gajbhiye, V.; Palanirajan, V. K.; Tekade, R. K.; Jain, N. K., Dendrimers as therapeutic agents: a systematic review. *JPP* **2009**, *61*, 989–1003.
20. Caminade, A. M.; Turrin, C. O.; Majoral, J. P., Phosphorous dendrimers in biology and nanomedicine: Syntheses, characterization, and properties. *Jenny Stanford Publishing* **2018**.
21. Mignani, S.; El Brahmī, N.; El Kazzouli, S.; Laurent, R.; Sonia Ladeira, S.; Caminade, A.-M.; Pedziwiatr-Werbicka, E.; Szewczyk, E. M.; Bryszewska, M.; Bousmina, M. M.; Cresteil, T.;

- Majoral, J.-P., Original multivalent gold(III) and dual gold(III)–copper(II) conjugated phosphorus dendrimers as potent antitumoral and antimicrobial agents. *Mol. Pharmaceutics* **2017**, *14*, 4087–4097.
22. Solassol, J.; Crozet, C.; Perrier, V.; Leclaire, J.; Beranger, F.; Caminade, A. M.; Meunier, B.; Dormont, D.; Majoral, J.-P.; Lehmann, S., Cationic phosphorus-containing dendrimers reduce prion replication both in cell culture and in mice infected with scrapie. *J. Gen. Virol.* **2004**, *85*, 1791-1799.
23. Wasiak, T.; Marcinkowska, M.; Pieszynski, I.; Zablocka, M.; Caminade, A. M.; Majoral, J. P.; Klajnert-Maculewicz, B., Cationic phosphorus dendrimers and therapy for Alzheimer's disease. *New J. Chem.* **2015**, *39* (6), 4852-4859.
24. Blattes, E.; Vercellone, A.; Eutamène, H.; Turrin, C. O.; Théodorou, V.; Majoral, J. P.; Caminade, A. M.; Prandi, J.; Nigou, J.; Puzo, G., Mannodendrimers prevent acute lung inflammation by inhibiting neutrophil recruitment. *Proc. Natl. Acad. Sci.* **2013**, *110* (22), 8795-8800.
25. Mignani, S.; El Kazzouli, S.; Bousmina, M.; Majoral, J.-P., Expand classical drug administration ways by emerging routes using dendrimer drug delivery systems: A Concise overview. *Adv. Drug Delivery Rev.* **2013**, *35*, 1316-1330.
26. Kana, B. D.; Karakousis, P. C.; Parish, T.; Dicke, T., Future target-based drug discovery for tuberculosis? *Tuberculosis (Edinb)* **2014**, *94*, 551–556.
27. Mohamad Sabbah, M.; Mendes, V.; Vistal, R. G.; Dias, D. M. G.; Monika Záhorská, M.; Mikušová, K.; Korduláková, J.; Coyne, A. G.; Blundell, T. L.; Abell, C., Fragment-Based Design of Mycobacterium tuberculosis InhA Inhibitors. *J. Med. Chem.* **2020**, *63*, 4749–4761.
28. Cavero, E.; Zablocka, M.; Caminade, A. M.; Majoral, J. P., Design of Bisphosphonate-terminated Dendrimers. *Eur. J. Org. Chem.* **2010**, *14*, 2759-2767.
29. Slany, M.; Bardaji, M.; Casanove, M.-J.; Caminade, A.-M.; Majoral, J.-P.; Chaudret, B., Dendrimer Surface Chemistry. Facile Route to Polyphosphines and Their Gold Complexes. *J. Am. Chem. Soc.* **1995**, *117*, 9764–9765.
30. Launay, N.; Caminade, A. M.; Lahana, R.; Majoral, J. P., A general synthetic strategy for neutral phosphorus-containing dendrimers *Angew. Chem., Int. Ed. Engl.* **1994**, *33*, 1589-1592.
31. Padié, C.; Maszewska, M.; Majchrzak, K.; Nawrot, B.; Caminade, A.-M.; Majoral, J.-P., Polycationic phosphorus dendrimers: synthesis, characterization, study of cytotoxicity, complexation of DNA, and transfection experiments. *New J. Chem.* **2009**, *33*, 318-326.
32. Badetti, E.; Caminade, A.-M.; Majoral, J.-P.; Moreno-Mañas, M.; Sebastián, R. M., Palladium(0) Nanoparticles Stabilized by Phosphorus Dendrimers Containing Coordinating 15-Membered Triolefinic Macrocycles in Periphery. *Langmuir* **2008**, *24*, 2090-2101.
33. Garcia, L.; Roglans, A.; Laurent, R.; Majoral, J.-P.; Pla-Quintana, A.; Caminade, A.-M., Dendritic phosphoramidite ligands for Rh-catalyzed [2+2+2] cycloaddition reactions: unprecedented enhancement of enantiodiscrimination. *Chem. Commun.* **2012**, *48*, 9248-9250.
34. Swinney, D. C.; Anthony, J., How were new medicines discovered? *Nat. Rev. Drug Discov.* **2011**, *10*, 507–519.
35. Mignani, S.; El Kazzouli, S.; Bousmina, M. M.; Majoral, J.-P., Dendrimer space concept for innovative nanomedicine: a futuristic vision for medicinal chemistry. *Prog. Polym. Sci.* **2013**, *38*, 993-1008.
36. Schirle, M.; Jenkins, J. L., Identifying compound efficacy targets in phenotypic drug discovery. *Drug Discov Today* **2016**, *21*, 82-89.
37. Payne, D. J.; Gwynn, M. N.; Holmes, D. J.; Pompliano, D. L., Drugs for bad bugs: confronting the challenges of antibacterial discovery. *Nat. Rev. Drug Discovery* **2007**, *6*, 29–40.

38. Mignani, S.; Rodrigues, J.; Roy, R.; Shi, X.; Cena, V.; El Kazzouli, S.; Majoral, J.-P., Exploration of biomedical dendrimer space based on in-vivo physicochemical parameters: Key factor analysis (Part 2). *Drug Discov. Today* **2019**, *24*, 1184-1192.
39. Mignani, S.; Rodrigues, J.; Roy, R.; Shi, X.; Ceña, V.; El Kazzouli, S.; Majoral, J.-P., Exploration of biomedical dendrimer space based on in-vitro physicochemical parameters: key factor analysis (Part 1). *Drug Discov. Today* **2019**, *24*, 1176-1183.
40. Laborde, J.; Deraeve, C.; Bernardes-Génisson, V., Update of Antitubercular Prodrugs from a Molecular Perspective: Mechanisms of Action, Bioactivation Pathways, and Associated Resistance. *ChemMedChem*. **2017**, *20*, 1657-1676.
41. Schrödinger Release 2020-2: Maestro, S., LLC, New York, NY **2020**.
42. Bochevarov, A. D.; Harder, E.; Hughes, T. F.; Greenwood, J. R.; Braden, D. A.; Philipp, D. M.; Rinaldo, D.; Halls, M. D.; Zhang, J.; Friesner, R. A., Jaguar: A high-performance quantum chemistry software program with strengths in life and materials sciences. *Int. J. Quantum Chem.* **2013**, *113*, 2110-2142.
43. Bowers, K. J.; Chow, E.; Xu, H.; Dror, R. O.; Eastwood, M. P.; Gregersen, B. A.; Klepeis, J. L.; Kolossvary, I.; Moraes, M. A.; Sacerdoti, F. D.; Salmon, J. K.; Shan, B.; Shaw, D. E., Scalable Algorithms for Molecular Dynamics Simulations on Commodity Clusters. *Proceedings of the ACM/IEEE Conference on Supercomputing (SC06) 2006 (November 11-17)*, Tampa, Florida (USA).
44. Harder, E.; Damm, W.; Maple, J.; Wu, C.; Reboul, M.; Xiang, J. Y.; Wang, L.; Luyman, D.; Dahlgren, M. K.; Knight, J. L.; Kaus, J. W.; Cerutti, D. S.; Krilov, G.; Jorgensen, W. L.; Abel, R.; Friesner, R. A., OPLS3: A Force Field Providing Broad Coverage of Drug-like Small Molecules and Proteins. *J. Chem. Theory Comput.* **2016**, *12*, 281-296.